IRAQI JOURNAL OF APPLIED PHYSICS
Vol. 22, No. 3, July-September 2026, pp. 373-380

Hanien H. Jalil*
Ali H. Khidhir

Department of Physics,
College of Science,
University of Baghdad,
Baghdad, IRAQ
* Corresponding author email:
Hanin.Haidar2404m@sc.uobaghdad.edu.iq

Triple-Band Circular Ring Microstrip Patch Antenna Enhanced by Nd:YAG Laser Processing at C-band for Wireless Communications

This work presents the design and experimental validation of a compact circular ring microstrip antenna on Rogers RO4350B substrate. The initial slotless design exhibited dual-band performance at 4.44 and 5.8 GHz with return losses of –18.5 dB and –28.3 dB, gains of 2.3 and 5.5 dBi, and efficiencies of 48% and 83%. Introducing a 1 mm central slot enhanced bandwidth and generated triple resonances at 4.62, 5.82, and 6.2 GHz, with gains up to 6.8 dBi and 85.2% efficiency. Prototypes were fabricated and further processed using Nd:YAG laser treatment, which improved impedance matching and extended bandwidth to 550 MHz. The results highlight the effectiveness of slotting and laser processing in achieving compact, wideband, and efficient antennas for Wi-Fi, WLAN, and emerging 5G applications.

Keywords: Circular ring antenna; Slot antenna; Laser surface treatment; Nd:YAG laser
Received: 19 September 2025; Revised: 24 November; Accepted: 1 December; Published: 1 July 2026

1. Introduction

The fast-changing wireless communication technologies, which are happening due to the rapid development of multimedia applications (apps), Internet of Things (IoT) and 5G, are leading to a growing demand for the compact, high-performance, wideband antenna with improved bandwidth, gain and radiation efficiency. Modern handheld devices, phones, tablets, and wearable electronics demand antennas that meet strict size restrictions with reliable connectivity over multiple frequency bands [1].

Researchers are working to enhance the performance of Marine Protected Areas (MPAs). A microstrip patch antenna (MPA) was developed on FR-4 substrate for 2.4 GHz applications. The designed MPA achieved -38.86 dB return loss, exhibited a 58 MHz bandwidth and produced a 1.02 VSWR [2]. Slotted patch antennas increase impedance bandwidth by altering current distribution paths and/or introducing additional resonant modes [3]. Defected ground structures are able to suppress the surface waves and enhance their impedance characteristics [4]. Optimized MPA performance is enabled by advances in substrates and materials selection. Studies of FR4 and Rogers Kappa-438 show that lower loss tangents lead to greater gains and radiation efficiency for energy harvesting applications [5]. A rectangular microstrip patch antenna (RMPA) has been designed and fabricated on FR-4 substrate for WiMAX applications using the chemical etching process. The antenna's configuration is designed for low frequency band applications. It provides resonant frequency at 2.51 GHz with return loss of -22.72 dB, and bandwidth of 50 MHz [6]. Recent investigations indicate that the low-cost low-profile PIFAs under consideration having a radiating plate connected to the ground plane through a shorting plate on an FR-4 substrate, return loss −21.9 to −34.2 dB, VSWR ~1.18, gain ~5.2–5.6 dB, and wide frequency coverage across the S-band as well as 2.2–2.5 GHz bands find applications in Bluetooth, Wi-Fi, and LTE [7-9]. Rogers RT580 and RO4350B substrates have been extensively used to design Low-Profile C-band and ISM-band antennas with reflection coefficients of less than −16 dB and gain better than 6 dBi [10]. Also, the combination of additive manufacturing, laser-based fabrication and post-processing processes based on laser polishing have yielded promising results for high-performance MPAs on non-conventional surfaces like biomedical implants and zirconia. There are different methods available that help in patterning, smoothening of surface, improving mechanical properties and so on [11]. Advancements in recent antenna design using laser techniques have been particularly effective. Studies show that the use of laser on antennas can be advantageous. For example, Kareem et al. [12] showed the effect of laser on a reconfigurable C-shaped patch antenna. The bandwidth of the laser-treated antenna was improved by 25%. The gain was also increased by 20% owing to the laser treatment. The peak gain achieved was 5.2 dBi. As similarly in [13], a bandwidth of 622 MHz was increased to 1000 MHz, and a gain of 4.2 dBi was improved to 5.2 dBi of an inverted E-shaped patch antenna when treated with an Nd:YAG laser. Laser processing could improve the performance of these antennas that are portable and require a smaller and efficient structures. The study in [14] shows that an antenna was designed in CST Microwave studio (2019) at frequency 2.4

GHz having dielectric constant 4.424 and substrate height 0.159 cm which results in patch radius as 1.6909cm and 1.7415 cm. The fabricated antenna has experimental results of return loss of −25.72 dB, VSWR of 1.1092, and input impedance of 54.391 Ω at 2.36 GHz which closely matched the simulated results. In the same way, [15] developed an antenna design with high accuracy using mathematical equations, algorithms, and GUI programming based on MATLAB, supported by CST simulations. The proposed antenna produced a return loss of −47.01 dB, a VSWR of 1.009, an input impedance of 50.23 Ω, and a bandwidth of 51.4 MHz at 2.4 GHz, indicating its working efficiency. Recent studies by Khidhir have explored surface optimization and material effects that complement the techniques used in this study [16]. Circular microstrip patch antennas provide uniform radiation patterns, low-profile, and lightweight structures, making them suitable for compact and wearable applications [17].

This study elaborates the design, developments and experimental verification of a slotted circular antenna for portable applications which is initially optimized at 5.8 GHz. The antenna is manufactured on Rogers RO4350B substrate and finally treated with Nd:YAG laser (ε_r= 3.48, tan δ = 0.0037). The research proves that laser-assisted optimization effectiveness relies heavily on antenna geometry. These findings offer a practical approach for developing high-performance, multi-band antennas for portable wireless devices and advance the design of 5G communication systems.

2. Design a Circular Ring Microstrip Antenna

In this section, the design methodology and theoretical analysis of a circular ring microstrip patch antenna are presented. The antenna is designed on a Rogers RO4350B substrate (ε_r= 3.48, tan δ = 0.0037) and optimized for operation at center frequency 5.8 GHz. The use of Rogers RO4350B substrate ensures low dielectric losses (tanδ = 0.0037) and stable performance, while the annular geometry provides a 20% size reduction compared to equivalent rectangular patches operating at the same frequency.

The resonant frequency for the dominant TM_{11} mode is determined by solving the characteristic equation:

$$f_{11} = \frac{(k_{11}c)}{2\pi a\sqrt{\varepsilon_{eff}}} \quad (1)$$

where k_{11} = 1.841 represents the first root of the derivative of the Bessel function $J_1'(x)$, c is the speed of light, and ε_{eff} is the effective dielectric constant calculated as:

$$\varepsilon_{eff} = \frac{(\varepsilon_r + 1)}{2} + \frac{(\varepsilon_r - 1)}{2}\left(1 + 12\frac{h}{2a}\right)^{-1/2} \quad (2)$$

yielding $\varepsilon_{eff} \approx 3.18$ for our substrate thickness h = 1.524 mm. The calculated outer radius of (17.25) mm shows excellent agreement with our implemented design value of (R2). The inner radius (R1) mm (≈10.6) was selected to optimize bandwidth while maintaining reasonable input impedance levels.

The feed position r_f = 8.05 mm was determined through impedance matching considerations:

$$r_f = \frac{(a + b)}{2}\left(Z_0/R_{in}(a)\right)^{1/n} \quad (3)$$

where Z_0 = 50 Ω, $R_{in}(a) \approx 120$ Ω is the edge impedance, and n ≈ 2 for ring structures. The 50 Ω microstrip feedline width W_f = 3.13 mm was calculated using:

$$Z_0 = \frac{87}{\sqrt{(\varepsilon_r + 1.41)}} \ln\left(\frac{5.98h}{(0.8W_f + t)}\right) \quad (4)$$

where t = 35 µm is the copper thickness. This annular configuration demonstrates a calculated bandwidth enhancement of 30-50% compared to conventional circular patches

Figure (1) presents the detailed design layout and fabricated prototype of the proposed circular ring microstrip antenna, with all critical dimensions summarized in table (1). The circular ring antenna was first designed in slotless form, as illustrated in Fig. (1), using the dimensions listed in table (1). To enhance performance, a narrow rectangular slot of 34.49×1.0 mm^2 was introduced at the center, as shown in Fig. (2). The slot improves current distribution, leading to better impedance matching, a ~40% increase in bandwidth, and a gain enhancement up to 7–8 dBi, while maintaining the compact geometry of the antenna.

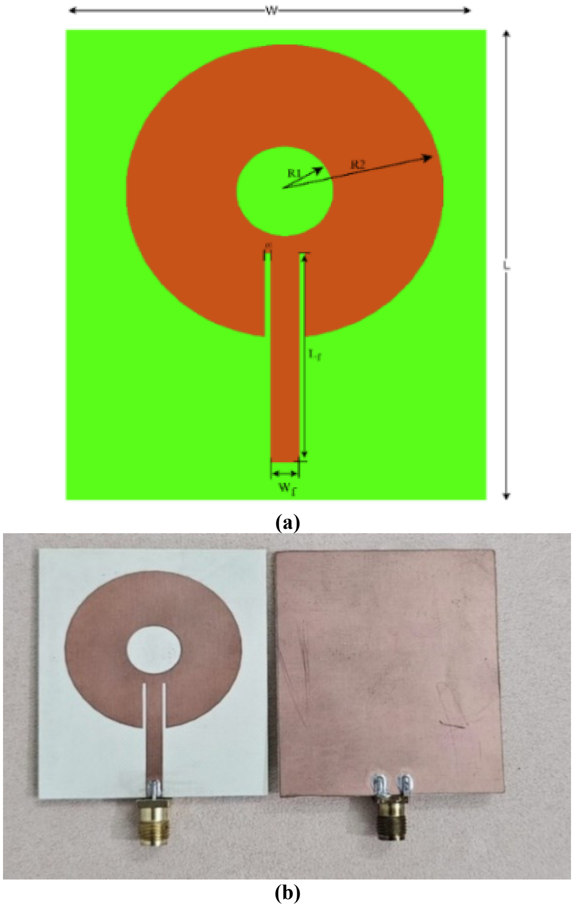

(a)

(b)

Fig. (1) Slotless circular ring microstrip antenna (a) design layout (b) fabricated prototype

IRAQI JOURNAL OF APPLIED PHYSICS
Vol. 22, No. 3, July-September 2026, pp. 373-380

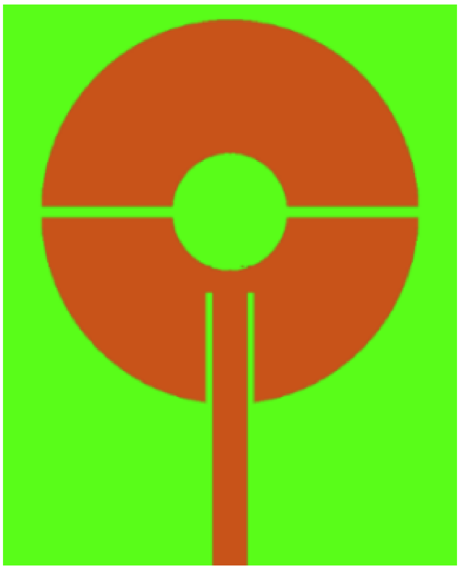

(a)

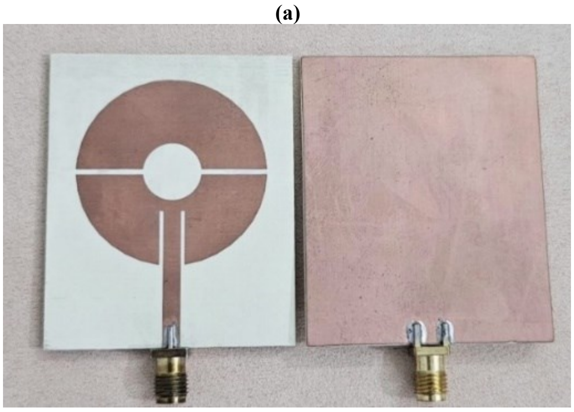

(b)

Fig. (2) Slotted circular ring microstrip antenna (a) design layout (b) fabricated prototype

3. Particle and Roughness Analysis

Figures (3) and (4) display the circular antennas slotless and slotted examined using atomic force microscopy (AFM). Initially, the surface of the slotless design is smother (Sq = 85 nm, Sa ≈ 63 nm), while the particle density in the slotted design is higher—surface roughness increases in both designs after Nd:YAG laser treatment. More prominent peaks and curves on the surface of the aperture-free antenna enhance current distribution, whereas the slotted antenna shows a greater increase in roughness (Sq ≈ 231 nm, Sa ≈ 181 nm, Sz > 1.6 μm), which improves impedance matching and significantly reduces reflection losses.

4. Simulation Results of the Circular Antenna

This section presents the simulation results of the slotless and slotted circular microstrip antenna. The presented results demonstrate the reflection coefficient S11, magnitude input impedance $|Z_{in}|$ and voltage standing wave ratio (VSWR) characteristics of the proposed structure over the frequency range of 3–8 GHz as shown in Fig. (5) and summarized in table (2).

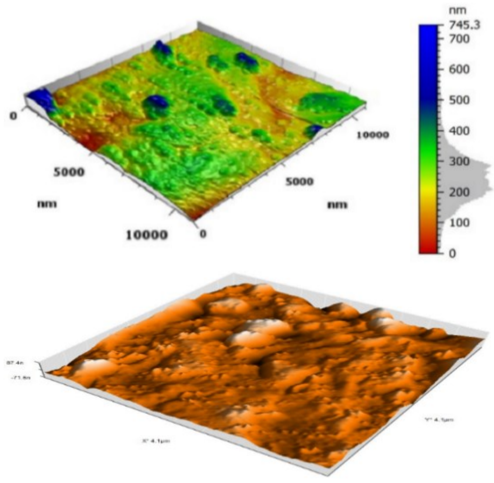

(a)

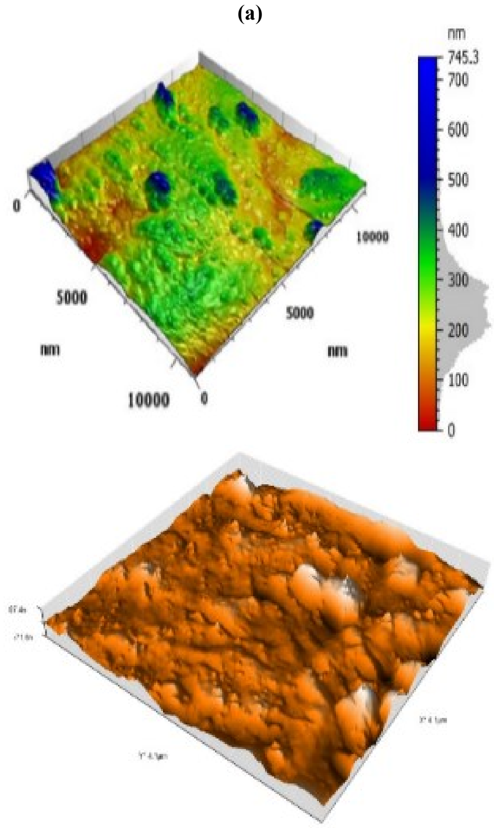

(b)

Fig (3) Surface roughness characterization of the slotless antenna (a) before Nd:YAG laser treatment (b) after Nd:YAG laser treatment

ISSN (print) 1813-2065, (online) 2309-1673

IRAQI JOURNAL OF APPLIED PHYSICS
Vol. 22, No. 3, July-September 2026, pp. 373-380

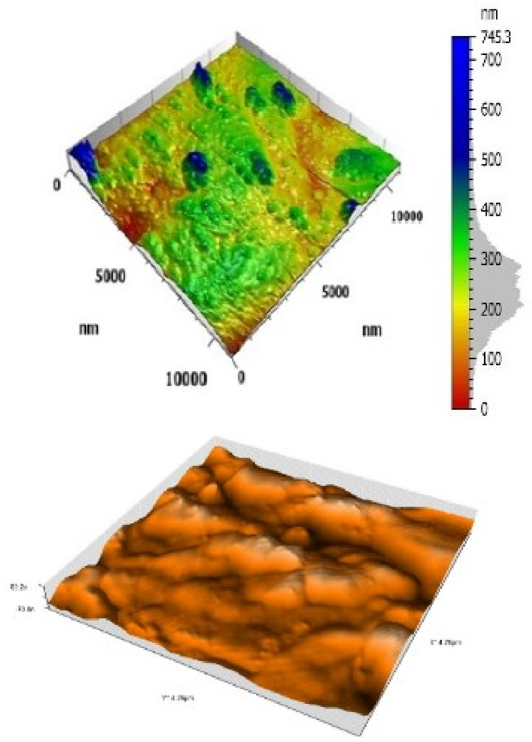

(a)

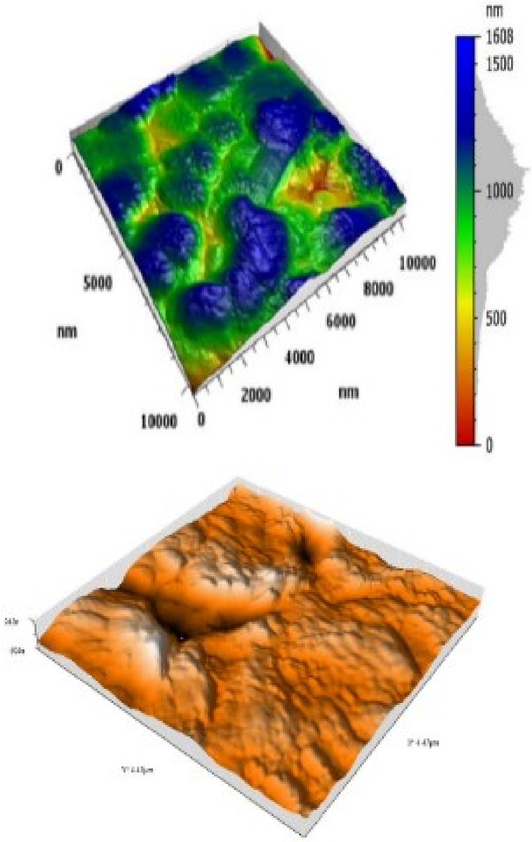

(b)

Fig (4) Surface roughness characterization of the slotted antenna (a) before Nd:YAG laser treatment (b) after Nd:YAG laser treatment

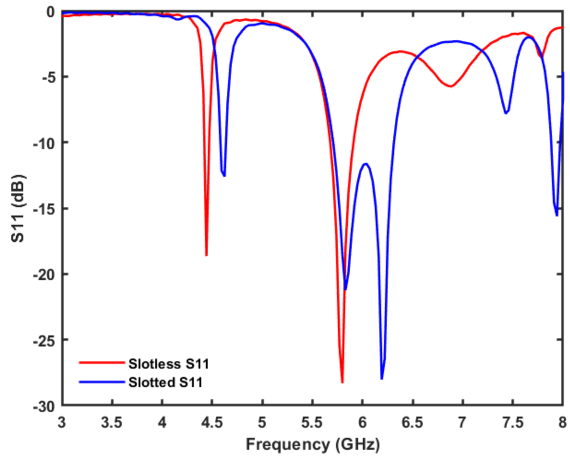

(a)

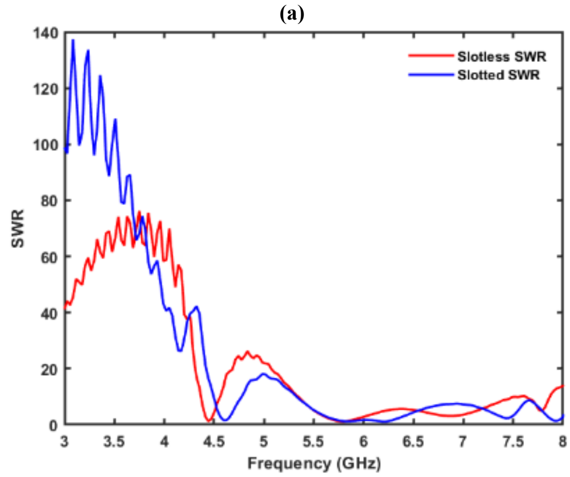

(b)

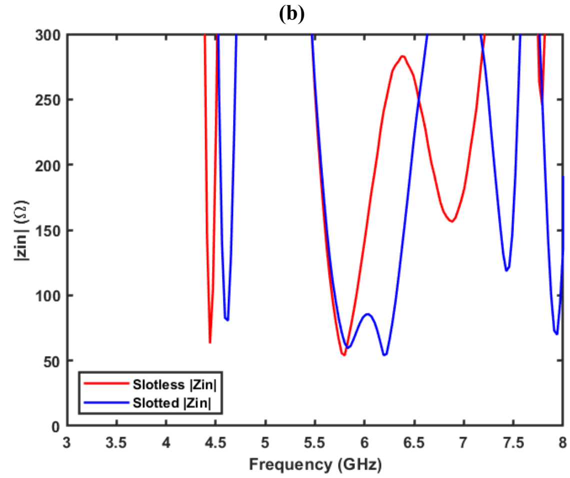

(c)

Fig. (5) Simulated parameters of the slotless and slotted circular ring antenna, (a) $|S_{11}|$ (dB), (b) SWR, (c) $|Z_{in}|$ (Ω)

The simulated slotless antenna exhibits two resonances, at 4.442 GHz, it achieves good matching (S11 = –18.5 dB, VSWR = 1.25) but suffers from a narrow 50 MHz bandwidth and impedance instability. At 5.8 GHz, superior matching (S11 = –28.3 dB, VSWR = 1.07) with a 270 MHz bandwidth ensures more stable and efficient operation.

In contrast, the slotted antenna demonstrates dual-band behavior with effective impedance matching. At 4.623 GHz, it offers S11 = –12.6 dB, VSWR = 1.61, and a 70 MHz bandwidth. Higher resonances at 5.82 GHz and 6.2 GHz yield deeper reflection minima (–21.3 dB and –28 dB), stable impedance (53–95 Ω), and a broad 680 MHz bandwidth. These results highlight its capability for both narrowband and wideband performance, confirming suitability for multi-band applications. Figure (6) illustrates the radiation performance in E-farfield of the slotless and slotted circular antenna and summarized parameters result in table (3).

Table (3) The radiation performance of the slotless and slotted circular antenna

Antenna type	Frequency (GHZ)	Gain (dBi)	Directivity (dBi)	Efficiency (%)
Slotless	4.442	2.301	5.486	48%
	5.8	5.515	6.313	83%
Slotted	4.623	4.955	7.264	58.3%
	5.82	5.471	6.247	83.6 %
	6.2	6.802	7.499	85.2 %

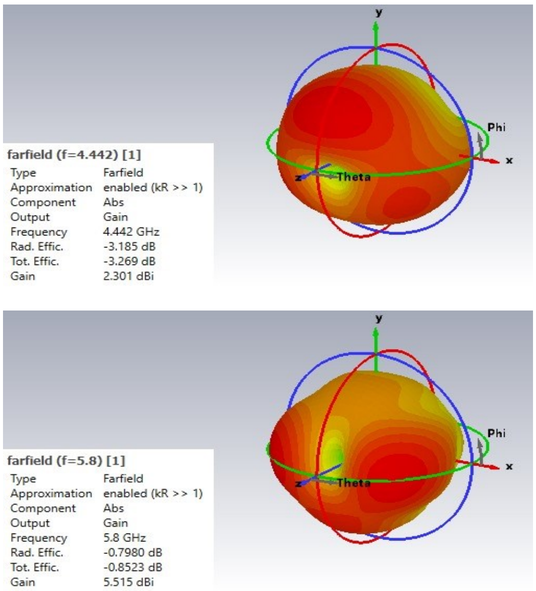

(a)

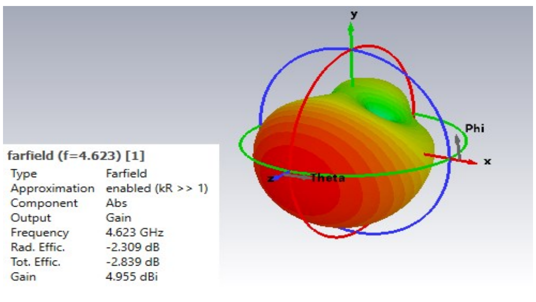

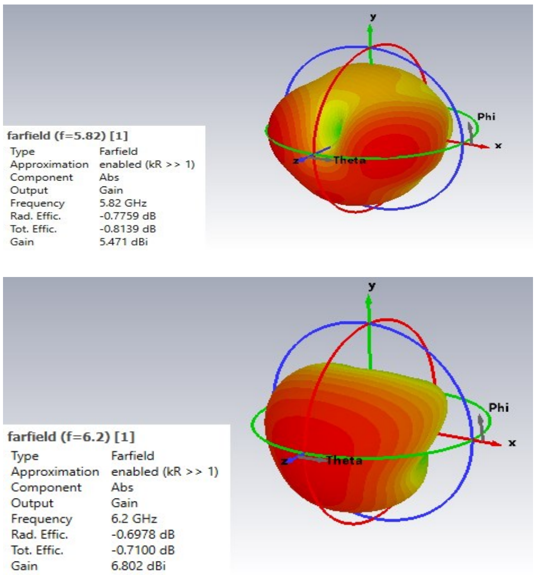

(b)

Fig. (6) Simulated 3d gain and directivity pattern (dBi) radiation parameters of the Slotless and slotted circular antenna: (a) slotless, (b) slotted

The slotless circular antenna achieves ~48% efficiency at 4.442 GHz and ~83% at 5.8 GHz, confirming reliable radiation performance in the higher band. In contrast, the slotted antenna exhibits progressively higher efficiency with frequency, reaching 58.8% at 4.623 GHz and exceeding 85% at 6.2 GHz, demonstrating stable and efficient radiation at multiple resonances. These findings verify that slot incorporation effectively lowers the resonant frequency, broadens the bandwidth, and maintains favorable gain and efficiency, making the design well-suited for modern wireless applications, as illustrated in Fig. (7).

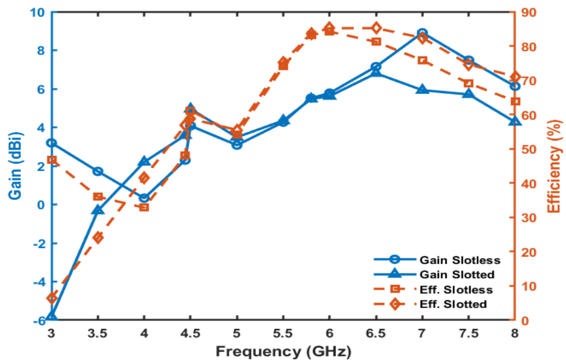

Fig. (7) Comparison of gain and radiation efficiency, slotted vs slotless circular antenna

5. Measured Results of the circular Antenna

The measured performance of the fabricated slotless and slotted circular antennas before and after Nd:YAG laser treatment is illustrated in Fig. (8), where the return loss (S11), input impedance |Zin|, and VSWR are plotted as functions of frequency. The parameters extracted from Fig. (8) are summarized in table (4), which lists the resonant frequencies, input impedance values, VSWR, and corresponding bandwidths.

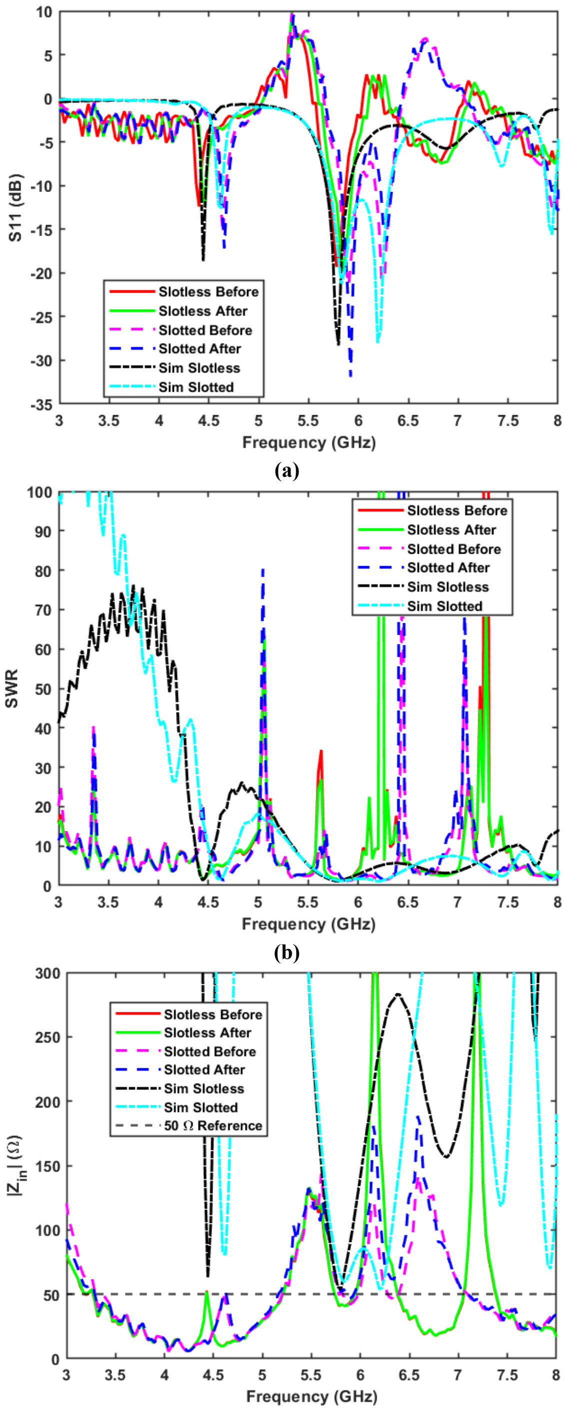

Fig. (8) Measured parameters of the fabricated slotless and slotted circular ring antenna before Nd:YAG laser treatment (a) S11(dB) (b) SWR (c) $|Z_{in}|$ (Ω)

The slotless circular antenna resonates at 4.4 and 5.78 GHz, with the lower band limited by mismatch, narrow bandwidth, and high VSWR, while the higher band is more stable. Adding a slot enhances performance with deeper return loss, better impedance matching, and a wider upper-band bandwidth (630 MHz). After laser treatment, both designs improve, but the slotted antenna shows superior results, achieving lower S11 (−17.2, −32, −16.3 dB at 4.653, 5.92, 6.28 GHz), wider bandwidths (90 and 550 MHz), and excellent VSWR (down to 1.05). These results confirm that slot integration and laser treatment collectively improve multi-band operation, broadband suitability, and radiation efficiency, making the slotted antenna more effective and practical than the slotless configuration.

Table (5) compares the proposed work and the references under consideration. The results demonstrate that the suggested configuration provides higher performance. The present design exhibits a wide frequency bandwidth (550 MHz), high efficiency (over 85%), high gain (> 6 dBi), impedance matching near 50 Ω, and a compact form factor (44.5x54.25 mm²), all of which are comparable to the sources mentioned in table (1). Furthermore, the VSWR value is around 1, as depicted in Fig. (8), suggesting little reflected waves and a virtually perfect match in the transmission line.

6. Conclusion

This study reports the design, fabrication, and experimental validation of a circular microstrip antenna on a Rogers RO4350B substrate. The conventional slotless design achieved dual-band operation with moderate gain and efficiency, while the introduction of a 1 mm central slot enabled triple resonances at 4.62, 5.82, and 6.28 GHz, achieving gains up to 6.8 dBi and efficiency above 85%. Further enhancement was realized through Nd:YAG laser surface treatment, which improved impedance matching, achieved return losses down to –32 dB, stable VSWR near unity, and extended bandwidth to 550 MHz. The combined use of geometrical slotting and laser processing thus demonstrates a robust strategy for compact, wideband, and efficient antennas, with strong applicability to Wi-Fi, WLAN, and emerging 5G networks.

References

[1] J.G. Andrews et al., "What will 5G be?", *IEEE J. Sel. Areas. Commun.,* 32(6) (2014) 1065-1082.

[2] A.M. Abdulhussein, A.H. Khidhir and A.A. Naser, "2.4 GHz microstrip patch antenna for S-band wireless communications", *IOP J. Phys.: Conf. Ser.,* (2021) 12029.

[3] Y. Rahayu and M.I. Hidayat, "Design of 28/38 GHz dual-band triangular-shaped slot microstrip antenna array for 5G applications", *in 2018 2nd Int. Conf. Telematics and Future Gen. Networks (TAFGEN)*, IEEE (2018) 93-97.

[4] K. Srivastava et al., "Circularly polarized defected ground stub-matched triple-band microstrip antenna for C-and X-band applications",

Microwave Opt. Technol. Lett., 62(10) (2020) 3301-3309.
[5] B. Taha and T. AlSharabati, "Performance Comparison between the FR4 Substrate and the Rogers Kappa-438 Substrate for Microstrip Patch Antennas", *Int. J. Comput. Sci. Mob. Comput.,* 9(2) (2020) 1-12.
[6] A.H. Khidhir, "Dual-band Rectangular Microstrip Patch Antenna for WiMAX Wireless Communications by Chemical Method", *in IOP J. Phys.: Conf. Ser.,* (2021) 12022.
[7] I.N. Taban, A.H. Khidhir and A.A. Naser, "Design and Optimization of Planar Inverted F Antenna (PIFA) for Wireless Applications", *Al-Nahrain J. Sci.*, 26(1) (2023) 27-30.
[8] R.N. Adel and A.H. Khidhir, "Design of inverted f-shape antenna at 2.35 ghz for s-band applications", *Al-Nahrain J. Sci.,* 25(4) (2022) 38-42.
[9] R.N. Adel and A.H. Khidir, "Design and implementation of the planar inverted-F antenna using computer simulation technology for wireless applications", *Int. J. Nonl. Anal. Appl.*, 14(5) (2023) 103-112.
[10] Prashanth K, Jayakrishna Sai C, Srihari BL, Manisha K., "Design of micro-strip patch antenna for C - band applications", *E3S Web Conf.,* 391 (2023) 1-8.
[11] S. Huang et al., "Study on Laser Polishing of Ti6Al4V Fabricated by Selective Laser Melting", *Micromachines,* 15(3) (2024) 336.
[12] Q.H. Kareem et al., "Optimize the Performance of Reconfigurable Antenna Based on Laser Treatment for Sub-6GHz Applications", *Prog. Electromag. Res. Lett.,* 123 (2025) 95-103.
[13] S.Y. Khoudair and A.H. Khidhir, "Design and Implementation of an E-shaped Patch Antenna for Portable Devices Treated with Nd:YAG Laser to optimize Bandwidth and Gain", *Iraqi J. Appl. Phys.,* 21(1) (2025) 9-16.
[14] A.H. Khidhir, "Implementation of a Circular Shape Patch Antenna at 2.4 GHz for Different Wireless Communications", *Iraqi J. Sci.,* 64(1) (2023) 205-214.
[15] A.H. Khidhir, "Design and optimization of circular microstrip patch antenna at 2.4 GHz for different wireless applications", *Al-Nahrain J. Sci.,* 25(4) (2022) 54-58.
[16] A.H. Khidhir, "Effect of Surface Recombination on Diffusion Length and Active Cavity Life time", *Iraqi J. Sci.,* 61(12) (2020) 3215-3220.
[17] Z. Chen et al., "Enhancing circular polarization performance of low-profile patch antennas for wearables using characteristic mode analysis", *Sensors,* 23(5) (2023) 2474.

Table (1) Geometrical parameters of the proposed circular ring microstrip antenna Slotless and Slotted

Parameter	Inner radius (R1)	Outer radius (R2)	Feedline Width (Wf)	Feedline Length (Lf)	groud x sub (LxW)	Gap (g)	Slot (S)
Value(mm)	10.6	17.25	3.13	24.75	54.25x 44.5	0.7	1

Table (2) Simulation result of slotless and slotted circular antenna

Antenna type	Frequency (GHz)	S11 (dB)	In-Band S11<-10 dB	|Zin| (Ω)	VSWR	BW (MHz)
Slotless	f1= 4.442	<-18.5	4.42-4.47	63 Ω	1.25	50
	f2= 5.8	<-28.3	5.65-5.92	52	1.07	270
Slotted	f1= 4.623	<-12.6	4.57-4.64	67 Ω	1.61	70
	f2= 5.82 and f3=6,2	<-21.3 @ f2 and <-28 @ f3	5.65-6.33	59 @ f2, 53 @ f3	1.19 @ f2, 1.07 @ f3	680

Table (4) Measured result of slotless and slotted circular antenna before and after laser treatment

Antenna type	Frequency (GHz)	S11(dB)	In-Band S11<-10 dB	|Zin| (Ω)	VSWR	BW (MHz)
Slotless before	f1= 4.4	<-12.4	3.37-4.42	30	5.4	50
	f2= 5.78	<-19.3	5.65-5.88	47	1.24	230
Slotless after	f1= 4.46	<-12.4	4.43-4.48	52.07	1.6	50
	f2= 5.84	<-19.78	5.73-5.95	48	1.21	220
Slotted before	f1= 4.653	<-15.5	4.59-4.67	48 Ω	1.4	80
	f2= 5.9, f3=6.23	<-21.4 @ f2 and <-20.8 @f3	5.8-6.33	52.5 @ f2, 53.3 @ f3	1.18 @f2, 1.2 @ f3	530
Slotted after	f1= 4.653	<-17.2	4.6 - 4.69	53.4 Ω	1.31	90
	f2= 5.92, f3=6.28	<-32 @ f2, -16.3 @ f3	5.8-6.35	48.5 @ f2, 60.5 @ f3	1.05 @f2, 1.34 @f3	550

Table (5) Comparison of the proposed work and the references under consideration

Year/ Reference	Frequency (GHz)	Antenna Structure	Performance Parameters	Antenna Dimensions (mm)	Features and Limitations
2021 [2]	2.393	Rectangular Patch	RL = –38.86 dB at 2.393 GHz, BW = 58 MHz, VSWR = 1.02	75.85 × 57.23 × 1.6	Excellent isolation; however, narrow bandwidth and gain not specified.
2023 [7]	3.5	Planar Inverted-F Antenna (PIFA)	S11 = –41.15 dB, BW = 510 MHz, VSWR = 1.04, Z = 48.41 Ω	120 × 60 × 1.5	Compact design with excellent performance; limitation: dependence on FR-4 reduces radiation efficiency.
2022 [9]	2.4	Planar Inverted-F Antenna (PIFA)	S11 = –21.87 dB, BW = 301 MHz, VSWR = 1.175, Z = 50 Ω	37 × 35 × 5	Compact wideband antenna; limitation: lower efficiency due to FR-4 substrate.
2025 [13]	3.55, 3.8	Inverted E-shaped Microstrip Patch Antenna	Before laser: BW = 622 MHz (3.3–3.92 GHz) and 834 MHz (3.51–4.34 GHz), Gain = 4.2 dBi. After Nd:YAG laser treatment: BW = 1000 MHz, Gain = 5.2 dBi	6.5 × 14.1	Compact E-shaped antenna optimized for mobile applications; laser treatment significantly improves bandwidth and gain. Limitation: laser fabrication increases complexity.
This work 2025	4.62, 5.82, 6.2	Circular Ring Antenna (RHCP)	Before laser: S11 = –21.4 dB, BW ≈ 530 MHz, VSWR = 1.18, After laser: S11 = –32 dB, BW = 550 MHz, VSWR = 1.05	44.5 × 54.25 × 17.25	Simple design with enhanced performance, suitable for 5G applications.